ELSEVIER

Agricultural and Forest Meteorology 93 (1999) 229–242

AGRICULTURAL AND FOREST METEOROLOGY

Wind and remnant tree sway in forest cutblocks. I. Measured winds in experimental cutblocks

Thomas K. Flesch*, John D. Wilson

Department of Earth and Atmospheric Sciences, University of Alberta, Edmonton, Alberta, Canada, T6G 2E3

Received 18 March 1998; accepted 15 September 1998

Abstract

New silvicultural techniques use unharvested forest strips to provide wind shelter in harvest cutblocks, and reduce windthrow for remnant trees. The objective of this paper was to characterise the winds across two such sheltered cutblocks: a narrow cutblock whose width (X_c) was 1.7 canopy heights (h), and a wide cutblock with $X_c = 6.1h$. Our focus was on the winds affecting understory trees, when the wind direction was across the cutblock width. Propeller and cup anemometer measurements were made along transects across the cutblocks, at height $z = 0.4h$. These data were normalised using windspeeds measured simultaneously in a much larger, nearby 'reference' clearing. In both cutblocks the best wind shelter was near the upwind forest edge, where the average cup windspeed (S) was reduced to approximately 20% of its value in the reference clearing, the average across-cutblock wind velocity (U) was approximately 10% of its clearing value, and the turbulent kinetic energy (TKE) was approximately 20% of its clearing value. Both U and S increased slowly with downwind distance (x) across the cutblocks. The pattern of turbulence was different, as TKE increased rapidly with x immediately downwind of the forest, then attained near-constancy beyond $x = 3h$ downwind of the forest edge (in the wide cutblock), at a value slightly above the clearing value. Based on these observations, we conclude that effective wind shelter in a cutblock occurs within three tree heights of the upwind forest edge (for understory trees of height $z \approx 0.5h$), where both the average wind velocity and the turbulence are reduced relative to their levels in larger clearings.

Keywords: Windthrow; Windbreaks; Forest winds; Forest management

1. Introduction

Large portions of the Canadian boreal forest have a predominantly aspen (*Populus tremuloides*) overstory with a white spruce (*Picea glauca*) understory. In some cases a selective harvesting of the mature aspen may be commercially worthwhile, leaving the 'released' spruce understory for future harvest. This 'two-stage' harvest system is also ecologically attractive, as it better maintains 'mixedwood' diversity compared with the traditional alternative of aspen clear-cutting.

An obstacle to this two-stage harvest is the susceptibility of the remnant spruce to windthrow (uprooting). Developed under a sheltered aspen canopy, individual spruce trees have poor wind stability, making them vulnerable to the increased wind exposure that accompanies aspen removal. Navratil et al. (1994) described

*Corresponding author. E-mail: thomas.flesch@ualberta.ca

0168-1923/99/$ – see front matter
PII: S0168-1923(98)00112-9

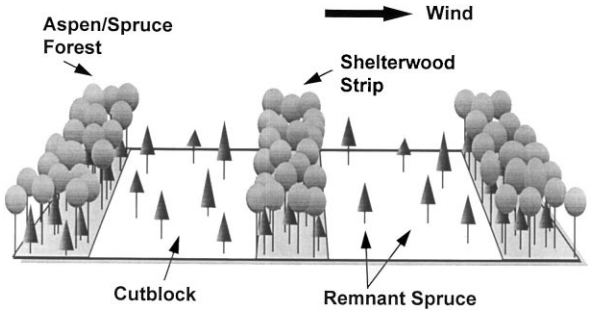

Fig. 1. Idealised view of shelterwood harvest system. Cutblocks are created by selectively harvesting the mature aspen overstory, leaving the spruce understory intact. Forest strips (shelterwood) separate the cutblocks, providing wind shelter.

the results of a two-stage harvest trial in western Canada, where aspen were harvested in large cutblocks, with dimensions of approximately 20 forest canopy heights (h). On average, 15–25% of the remnant spruce taller than $0.4h$ were lost to windthrow within 3 years of aspen harvest. These trials were on dry soils, and higher even losses would be expected on the wetter soils common to the mixedwood region of Canada. Therefore, the development of silvicultural techniques to provide wind protection is deemed essential for the success of two-stage harvest systems.

One proposed solution to the windthrow problem is a shelterwood system. In a shelterwood design (Fig. 1) the aspen is harvested in a series of narrow cutblocks, separated by unharvested forest strips (shelterwood). The cutblocks are oriented perpendicular to the expected direction of maximum wind. The forest strips are then analogous to agricultural windbreaks, and the expectation is that they will provide wind shelter for the remnant spruce in the cutblocks.

McNaughton (1989) described the general features of wind flow behind a thin windbreak of height h. Immediately downwind of the windbreak is a 'quiet zone' where the average wind velocity and the turbulence (conveniently characterised by the turbulent kinetic energy, TKE) are reduced relative to the 'ambient' levels far upwind. This quiet zone lies below a line that extends roughly from the top of the windbreak to the ground about $8h$ behind the windbreak. Further downwind, and above the quiet zone, lies a 'wake zone', where the TKE is enhanced over ambient levels (although the average wind velocity is still reduced from ambient). Still further downwind there is an eventual recovery to the ambient (i.e., upstream wind conditions).

Does this pattern exist in forest cutblocks? The observations of Gash (1986), Raupach et al. (1987), and Liu et al. (1996) suggest it does – if 'ambient' in these cases is defined by the wind condition in a clearing far *downwind* of the forest. In these studies one can observe a quiet zone immediately downwind of the forest, followed by a wake zone. This is encouraging from a windthrow protection standpoint, as it suggests that narrow cutblocks will experience wind shelter, particularly if their width is limited to the dimensions of the quiet zone. However, a series of forest-cutblock strips has a more complicated geometry than either an isolated windbreak, or an isolated forest-clearing interface. It is possible to imagine complex flow patterns where the quiet and wake zones are altered in location, or are no longer appropriate descriptions of cutblock flow.

A micrometeorological field experiment was undertaken with the goal of providing a theoretical basis for understanding the windthrow protection afforded by shelterwood cutblocks. Our objective was quite specific: to quantify windthrow protection available for an isolated remnant understory spruce, when winds are oriented across the cutblock. In this, the first part of the study, we describe winds across two differently sized cutblocks. We were particularly interested in whether a common flow pattern exists across cutblocks of different dimensions and across cutblocks having different upwind and downwind forest features. The second phase of the work (Flesch and Wilson, 1999) relates wind velocity statistics to remnant tree sway, so that cutblock wind shelter can be quantified in terms of tree sway. In the third phase of the study, a wind flow model (Wilson and Flesch, 1999) was developed to generalise our measurements in a way that allows spatial mapping of windthrow hazard for arbitrary cutblock designs.

2. Field measurements

2.1. The Hotchkiss silviculture experiment

A silvicultural experiment in Alberta, Canada is examining shelterwood designs for effectiveness at reducing remnant spruce windthrow. The project site

is approximately 30 km northwest of Manning, at a location called Hotchkiss River. The area is classified as boreal mixedwoods, having a predominantly aspen overstory of 20–25 m in height, with a significant white spruce understory averaging 10 m in height. The terrain is gently rolling.

During the initial harvest, aspen and mature spruce were removed from long rectangular cutblocks, whose width ranged from approximately 40–150 m, and whose length varied from approximately 500–1000 m. The cutblocks were oriented perpendicular to the direction of the expected maximum winds (westerly). Remnant spruce density in the cutblocks varied according to the density of the original understory.

2.2. Wind measurements

Two cutblocks were selected for study (Fig. 2(a) and Fig. 2(b)): a wide cutblock with width (X_c) = 140 m (studied in 1994 and 1995), and a narrow cutblock with $X_c = 40$ m (studied in 1996 and 1997). These cutblocks were 500 and 700 m in length, respectively. Each was the furthest east in a series of nominally identical cutblocks, which were separated by forest strips of about the same width (X_f) as the cutblocks (e.g., the 140 m wide cutblock was bordered upwind by a 150 m wide forest strip: $X_c \approx X_f$). We defined x as the across-cutblock coordinate (very nearly east–west), y as the along-cutblock coordinate, and z as a vertical coordinate. The origin $x = 0$ lies at the westward edge of the test cutblock, with x increasing toward the east (downwind for most of our discussion). Wind measurements were made in each test cutblock, along east–west transects sited where the residual spruce density was low (we cut down the few trees that might otherwise have created wind anomalies along the transect). The canopy height (h) was approximately 23 m.

In 1994 towers were placed at $x/h = -0.8$, 1.0, 2.1, 3.2, 4.3, 5.4, and 7.2 in a transect across the wide cutblock (Fig. 2(a)); the cutblock boundaries lying at $x/h = 0$ and 6.1. Cup anemometers (Climet Instruments Co., model 011B) were placed on each tower at $z = 9$ m ($z/h = 0.4$) to measure the average cup windspeed (S). From October to November in both 1994 and 1995, hourly S were recorded, encompassing a range of wind directions and speeds. The S measure-

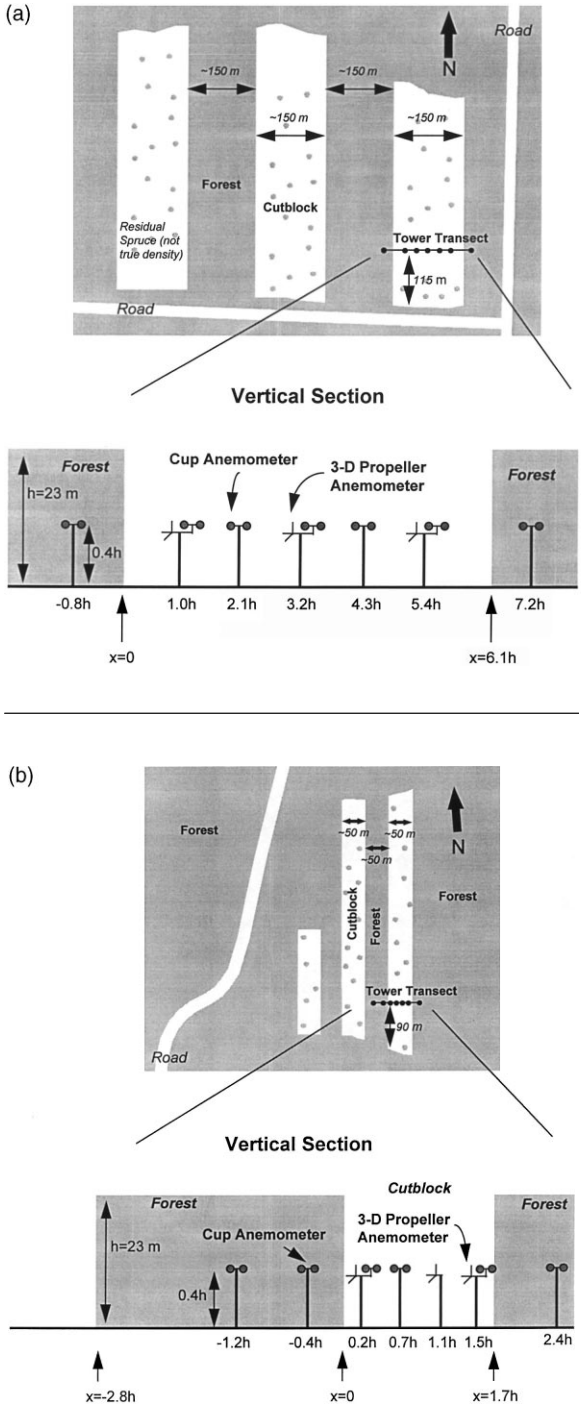

Fig. 2. (a) Location of wind measurements in the wide cutblock. We have illustrated cup anemometers on all towers, and 3–D propellers at $x/h = 1.0$, 3.2, and 5.4. (b) Location of wind measurements in the narrow cutblock.

ments were corrected for cup overspeeding (see Appendix).

Three-dimensional (3-D) propeller anemometers (R.M. Young Co., Gill UVW anemometer) were operated during periods of high winds oriented across the cutblock (westerly winds). In 1994 the propellers were placed at $x/h = 1.0$, 3.2, and 5.4 (at $z = 9$ m). In 1995 they were placed at $x/h = -0.8$, 3.2, and 7.2. Average windspeed and direction at $x/h = 3.2$ were used to trigger propeller sampling, which lasted 15 min with a 5 Hz sampling frequency. A datalogger (Campbell Scientific Inc., CR–7X) recorded the measurements. Propeller data were recorded as a voltage time series, and later converted to velocities according to Horst (1972), correcting for the imperfect cosine response of these anemometers. Six measurement periods were selected for analysis in 1994, and five in 1995 (Table 1).

In 1996 the towers were moved to the narrow cutblock and placed at $x/h = -1.2$, -0.4, 0.2, 0.7, 1.1, 1.5, and 2.4 (Fig. 2(b)); the cutblock boundaries lying at $x/h = 0$ and 1.7. Cup anemometers were placed on six of the towers (excluding $x/h = 1.1$), and hourly S were recorded in October and November 1996. The 3-D propeller anemometers were placed at $x/h = 0.2$, 1.1, and 1.5. Propeller measurement periods lasted 30 min (the increased duration from 1995 was due to increased data storage capability). Five periods were selected for analysis (Table 1). In the fall of 1997, the propellers were placed at $x/h = -1.2$ and 0.7, and two 30 min periods were recorded.

We used u, v, w to denote the instantaneous across-cutblock velocity (x direction), along-cutblock velocity (y direction), and the vertical velocity, respectively. We will write, for example, an instantaneous velocity $u = U + u'$, where U is the time average velocity, and u' is the instantaneous departure from average. For each velocity time series measured with the propellers, we calculated the following statistics (the angle brackets $\langle\ \rangle$ denote a time average):

- average velocities, denoted U, V, and W;
- average cup windspeed, $S = \langle (u^2 + v^2)^{1/2} \rangle$;
- velocity standard deviations, denoted σ_u, σ_v, and σ_w;
- turbulent kinetic energy, $\mathrm{TKE} = (\sigma_u^2 + \sigma_v^2 + \sigma_w^2)/2$;
- velocity skewness, denoted Sk_u, Sk_v, and Sk_w (e.g., $\mathrm{Sk}_u = \langle u'u'u' \rangle / {\sigma_u}^3$);
- velocity kurtosis, denoted Kt_u, Kt_v, and Kt_w (e.g., $\mathrm{Kt}_u = \langle u'u'u'u' \rangle / {\sigma_u}^4$);

Table 1
Propeller anemometer measurement periods used in the study

Number	Cutblock width (m)	Date	Time of the day	S_{clr} (m s^{-1})	Wind direction[a]	Gill UVW locations
W–1	6.1h	27 October 1994	13:45–14:00	6.41	3°	x/h = 1.0, 3.2,5.4
W–2	6.1h	28 October 1994	10:15–10:30	4.85	4°	x/h = 1.0, 3.2, 5.4
W–3	6.1h	28 October 1994	11:45–12:00	4.97	16°	x/h = 1.0, 3.2, 5.4
W–4	6.1h	28 October 1994	12:00–12:15	5.86	25°	x/h = 1.0, 3.2, 5.4
W–5	6.1h	4 November 1994	11:00–11:15	6.21	3°	x/h = 1.0, 3.2, 5.4
W–6	6.1h	18 November 1994	16:15–16:30	5.21	−16°	x/h = 1.0, 3.2, 5.4
W–7	6.1h	26 October 1995	11:45–12:00	3.69	10°	x/h = −0.8, 3.2, 7.2
W–8	6.1h	26 October 1995	12:00–12:15	3.70	24°	x/h = −0.8, 3.2, 7.2
W–9	6.1h	26 October 1995	15:45–16:00	4.21	−7°	x/h = −0.8, 3.2, 7.2
W–10	6.1h	26 October 1995	16:15–16:30	3.47	−14°	x/h = −0.8, 3.2, 7.2
W–12	6.1h	26 October 1995	17:30–17:45	4.39	−15°	x/h = −0.8, 3.2, 7.2
N–1	1.7h	7 October 1996	11:00–11:30	4.71	4°	x/h = 0.2, 1.1, 1.5
N–2	1.7h	11 October 1996	09:00–09:30	7.50	−13°	x/h = 0.2, 1.1, 1.5
N–3	1.7h	11 October 1996	10:00–10:30	7.06	−10°	x/h = 0.2, 1.1, 1.5
N–4	1.7h	11 October 1996	12:00–12:30	6.89	−3°	x/h = 0.2, 1.1, 1.5
N–5	1.7h	11 October 1996	14:00–14:30	7.82	0°	x/h = 0.2, 1.1, 1.5
N–6	1.7h	26 September 1997	13:00–13:30	4.94	−26°	x/h = −1.2, 0.7
N–7	1.7h	26 September 1997	13:30–14:00	4.94	−26°	x/h = −1.2, 0.7

[a] 0° is across the cutblock (westerly).

Simultaneous with our cutblock measurements, average cup windspeed and wind direction (hourly averages) were measured in a large 'reference' clearing 5 km from the cutblocks. This clearing was irregularly shaped, with a diameter of roughly 1 km. A cup anemometer (Met-One, Model 013A) was placed at $z = 9$ m on a tower that was 12–30h from the forest edge. The case in which we were most interested (west winds) put the tower 20h downwind of the forest edge, with the clearing extending approximately 20h further downwind of the tower. Throughout this work we will use the clearing cup windspeed (S_{clr}) as a velocity scale to normalise our in-cutblock data, to permit an assessment of the windiness of the cutblocks *relative to* an essentially open region (presumably the worst case scenario for remnant windthrow). We will also use S_{clr} and the wind direction in the clearing to derive a reference across-cutblock wind velocity (U_{clr}). During November 1995, a 3–D propeller was placed in the reference clearing (at $z = 9$ m), and ten 15 min measurement periods were used to characterise the turbulence there.

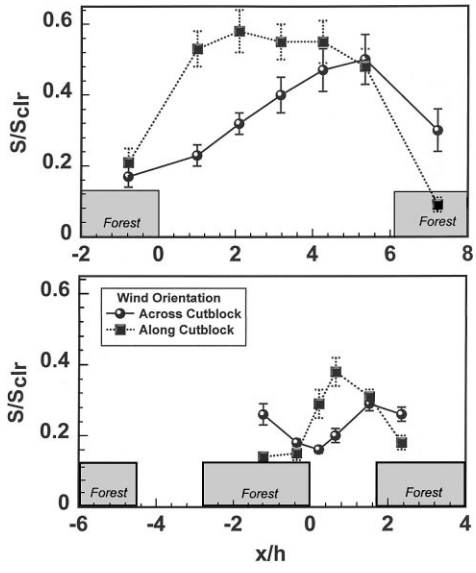

Fig. 3. Average cup windspeed (S), scaled on windspeed in the nearby reference clearing (S_{clr}), and plotted versus position (x/h) in the wide cutblock (top) and the narrow cutblock (bottom). The two lines are for ambient winds oriented across the cutblock (average wind direction along x, $\pm 30^\circ$) and along the cutblock length (average wind direction along y, $\pm 30^\circ$). The 'error bars' surrounding each observation are $\pm$ one standard deviation.

3. Measured winds in forest cutblocks

3.1. Average cup windspeed

Average cup windspeed (S) within our study cutblocks was significantly reduced from that in the nearby reference clearing (S_{clr}), as illustrated in Fig. 3. During windy periods ($S_{clr} > 3$ m s^{-1}) S/S_{clr} ranged from 0.12 to 0.64, depending on the wind direction and on location in the cutblock. As expected, S/S_{clr} increased with increasing distance from the upwind forest edge. The most effective sheltering (lowest spatial average S/S_{clr} along our transect) occurred when the wind was oriented directly across the cutblock, which at any location, minimized the distance to the upwind forest. For example, when the wind was oriented across the wide cutblock (along the x direction, $\pm 30^\circ$) S/S_{clr} in the cutblock ranged from 0.23 at the upwind tower to 0.51 at the downwind tower, but when the winds were oriented along the cutblock length, this speed range increased to between 0.47 and 0.53 (Fig. 3). This seems to confirm the premise of the Hotchkiss silviculture trials: that maximum shelter occurs when the wind is oriented across the cutblocks. There was a concern, in terms of windthrow, that wind channelling might occur when winds are oriented along the cutblock length, with $S/S_{clr} > 1$. We saw no sign of this. From now on, our focus will be on the case where the wind is oriented directly across the cutblock – the optimum case for wind shelter.

With the wind oriented across the cutblocks, the pattern of S was qualitatively the same as found behind an isolated windbreak: S was at a minimum near the windbreak, and increased slowly with downwind distance (Fig. 3). In the forest immediately upwind of both cutblocks, we observed an average S/S_{clr} of approximately 0.17. We cannot say whether the minimum S was at the forest edge ($x = 0$), or just upwind or downwind of the edge. We saw an almost linear increase in S with distance from the forest edge, so that S/S_{clr} reached approximately 0.5 at $x/h = 5.4$ in the wide cutblock, and 0.3 at $x/h = 1.5$ in the narrow cutblock. In each cutblock the maximum S occurred at the farthest downwind measurement location.

3.2. Average wind velocity

When we restrict our attention to winds oriented across the cutblocks ($V = 0$), we might expect the average along-wind velocity (U) to be very similar to S. But since $S = \langle (u^2 + v^2)^{1/2} \rangle$, it follows that S increasingly exceeds U as σ_v increases, or the proportion or magnitude of flow reversal (i.e., $u < 0$) increases. Far above a homogeneous surface, the difference between S and U is generally small. We observed a different situation in the cutblocks.

In the wide cutblock, U/U_{clr} ranged from approximately 0.1 in the upwind forest to 0.42 at the downwind cutblock tower (Fig. 4). These values were smaller than the corresponding S/S_{clr} ratios, although the spatial pattern was similar. This was not the case for the narrow cutblock. While S was at a minimum near $x = 0$, U was near its maximum there. And while S almost doubled across the cutblock, U showed less change. These differences were the result of a large

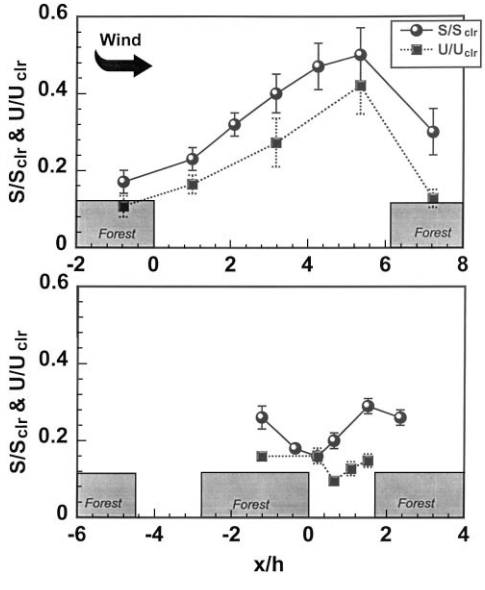

Fig. 4. Average cup windspeed (S) and across-cutblock velocity (U), scaled on their values in the reference clearing (S_{clr} and U_{clr}), plotted versus position (x/h) in the wide cutblock (top) and the narrow cutblock (bottom). Winds were oriented across the cutblock (along x direction, $\pm 30^{\circ}$). The S are from 9 hours (wide cutblock) and 6 hours (narrow cutblock) of cup anemometer measurements. The U values are from 1 to 2.5 hours of 3–D propeller measurements. The 'error bars' surrounding each observation are $\pm$ one standard deviation.

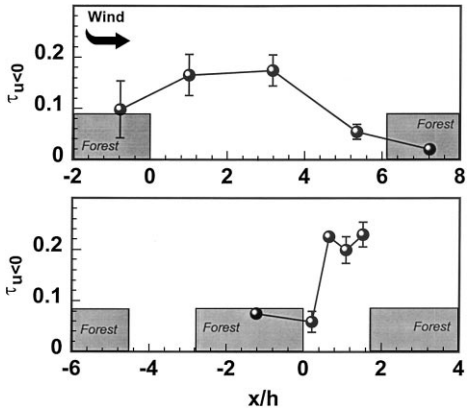

Fig. 5. Average time fraction of flow reversal ($\tau_{u<0}$) in the wide cutblock (top) and narrow cutblock (bottom). The 'error bars' surrounding each observation are $\pm$ one standard deviation.

rise in the turbulence intensity with increasing x, and intermittent flow reversal. Fig. 5 shows the time fraction when $u < 0$ in the cutblocks ($\tau_{u<0}$). This varied from 0 to 0.17 in the wide cutblock, and from 0.06 to 0.23 in the narrow cutblock.

The U deceleration in the upwind portion of the narrow cutblock indicated mass convergence, and in view of the continuity equation (in its 2–D form, assuming $\partial/\partial y = 0$)

$$\frac{\partial U}{\partial x} + \frac{\partial W}{\partial z} = 0$$

suggested updrafts on average over the upwind portion of the cutblock. Our observations did show $W > 0$ at the upwind tower locations, particularly in the narrow cutblock (although our W observations are prone to uncertainty due to the difficulty in levelling the anemometers).

3.3. Turbulence statistics[1]

3.3.1. Turbulent wind velocities and TKE

Besides providing shelter in terms of the *average* windspeed, the cutblocks provided an environment of reduced wind-*variability* (turbulence) compared with large clearings – at least over part of the cutblocks.

[1]Statistics from propeller anemometers are subject to errors from poor high frequency response and stalling. We believe these errors are small in this experiment (see Appendix).

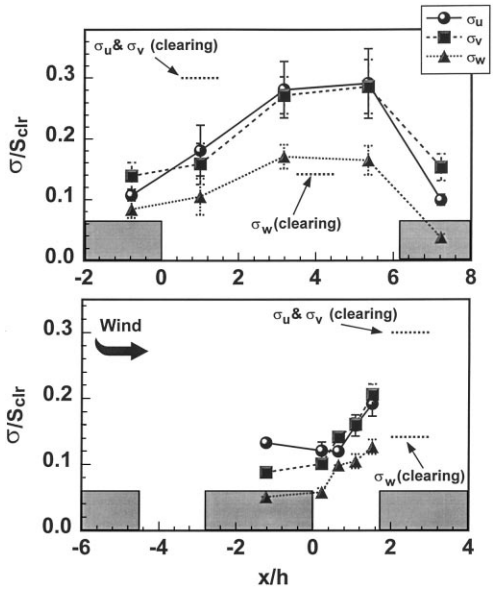

Fig. 6. Velocity standard deviations (σ_u, σ_v, σ_w), scaled on cup windspeed in the nearby reference clearing (S_{clr}), plotted across the wide cutblock (top) and the narrow cutblock (bottom). The 'error bars' surrounding each observation are ± one standard deviation. Values of σ_u/S_{clr}, σ_v/S_{clr}, and σ_v/S_{clr} in the reference clearing are shown by the level dashed lines (which are not at their proper location on the x axis).

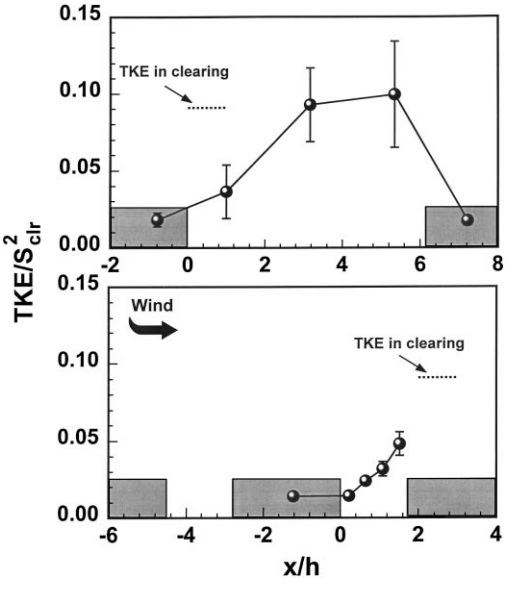

Fig. 7. Average turbulent kinetic energy (TKE), scaled on cup windspeed in the nearby reference clearing (S_{clr}), across the wide cutblock (top) and the narrow cutblock (bottom). The 'error bars' surrounding each observation are ± one standard deviation. Also shown (by the level dashed line) is TKE/S^2_{clr} in the reference clearing.

Fig. 6 shows the velocity standard deviations (σ_u/S_{clr}, σ_v/S_{clr}, σ_w/S_{clr}) across the two cutblocks. Values of σ_u and σ_v were statistically identical in the cutblocks, with σ_w about 60% of σ_u and σ_v. The spatial patterns of σ_u, σ_v, and σ_w were similar, and the turbulent kinetic energy (TKE) shows this pattern (Fig. 7). The TKE in the wide cutblock rose from 19% of the reference clearing value at the upwind forest edge, to plateau at more than 100% of the clearing value for $x/h > 3$. In the narrow cutblock, the steep increase in TKE was sustained all the way across the cutblock, although the TKE never reached the level found in the reference clearing.

This pattern of turbulence generally corresponds to that found behind a thin windbreak (see review by McNaughton, 1989). The region from $0 < x/h \leq 3$ can be labelled a 'quiet zone', where the turbulence was reduced from clearing levels. Downwind of this was a 'wake zone', where the turbulence level exceeded that found in the clearing. The enhanced turbulence originates with the strong vertical wind shear concentrated near the top of the canopy at the upwind forest edge (which results in enhanced TKE production). Raine and Stevenson (1977) broadly divided the quiet and wake zones behind a thin windbreak with a line running from the top of the windbreak to the ground at $x/h = 8$. Based on this general rule, we should have found the transition from quiet to wake zones occurring at $x/h = 4.8$ (at $z/h = 0.4$), not at $x/h \approx 3.0$. This is consistent with McNaughton's (1989) speculation that the quiet zone behind a forest edge may be less extensive than that behind a typical thin agricultural windbreak, because the greater level of turbulence over a rough forest (compared with over typical agricultural land) increases the rate of vertical spread of the wake zone from the forest edge.

3.3.2. Skewness and kurtosis

Wind flow in plant canopies is often characterised as a temporally dominant 'quiescent' regime with intermittent gusts (Finnigan and Raupach, 1987). Velocity skewness (Sk) is often taken as indicative of gust intermittency. A positive Sk_u, which is a characteristic of canopy flow, is the result of an

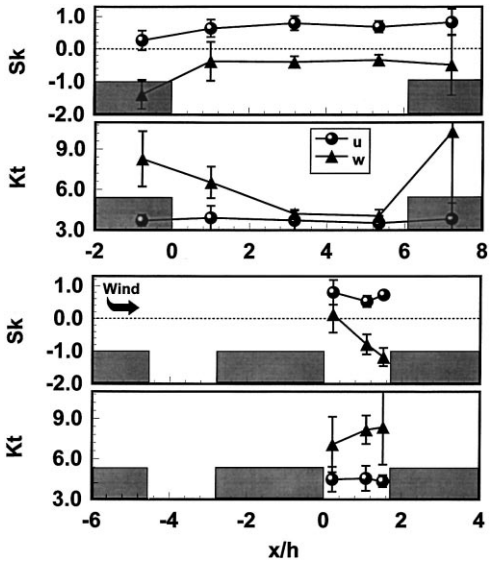

Fig. 8. Average skewness (Sk) and kurtosis (Kt) for u and w across the wide cutblock (top two graphs) and the narrow cutblock (bottom two graphs). The 'error bars' surrounding each observation are ± one standard deviation.

asymmetric probability density function (PDF), with a long 'tail' toward large u values (gusts). If windthrow is the result of short duration gusts, Sk may be useful in identifying areas prone to wind damage: a larger Sk_u will correspond to greater extreme u values for a given σ_u.

Fig. 8 illustrates Sk_u and Sk_w in our study cutblocks. We have less confidence in these statistics compared with averages and standard deviations, due both to propeller errors (discussed in the Appendix), and to the known need for longer averaging intervals to determine higher-order statistics. Within the cutblocks the average Sk_u varied from 0.5 to 0.8, while Sk_w fell between -1.2 and 0. These were within the range commonly observed within forest canopies (e.g., Baldocchi and Meyers, 1989; Amiro, 1990), indicating the occasional occurrence of high speed gusts originating above the canopy (with $u' > 0$, $w < 0$). Flow was also marked by Kt exceeding 3, the value for a Gaussian PDF (Fig. 8). This is consistent with a 'two-state' canopy flow, dominated by a quiescent regime but punctuated by infrequent gusts giving a broad PDF tail. The 'scatter' in our Sk and Kt observations, and the likelihood of measurement errors makes it difficult to discern any spatial pattern across the cutblocks. The apparently modest spatial variation in Sk_u and Kt_u seems to rule out the possibility of hidden 'hot spots' in the cutblocks: there is little reason to suspect the existence of cutblock locations more prone to intense gusts than is indicated from an assessment merely of U and σ_u.

3.4. Throughflow or recirculating flow?

Observations by Bergen (1975), Weiss and Allen (1976), and Raupach et al. (1987) suggest that the wind pattern across a forest clearing varies temporally between direct throughflow and recirculating flow. In throughflow, clearing streamlines everywhere are oriented with the above canopy streamlines, and the wind flows *into* the downwind forest at all height levels. Recirculating flow is marked by a standing vortex (rotor) within the clearing, with reverse flow near the ground. In smaller clearings this rotor may span the full width of the clearing, while it may be confined to the areas near the forest edge in large clearings.

The time spent in throughflow- and recirculation-states appears to depend on forest porosity, with increased porosity leading to increased dominance of the throughflow-state, and more intermittent recirculation (Raupach et al., 1987). Did recirculation occur in our cutblocks? Our limited observations make this question difficult to answer. Bergen (1975) examined wind flow across a narrow pine clearing ($X_c = 1$) and classified the flow as recirculating 25% of the time. Our leafless aspen forest was almost certainly less dense that Bergen's, and on that basis we might expect less frequent recirculation.

What would recirculation 'look' like in our observations? We focused on our narrow cutblock, where rotors were expected to have features similar to those observed by Bergen: they would span the width of the cutblock, and have an average duration of 10 to 20 s before a return to throughflow. Our data was broken into 10 s blocks, and the fraction (τ_{recir}) of these blocks having possible recirculation was calculated: the recirculation-state characterised by the requirement of updrafts at the upwind cutblock tower, and downdrafts at the downwind tower (10 s blocks were classified as having updrafts or downdrafts when $|W| > 0.2\ m\ s^{-1}$). We calculated $\tau_{recir} = 0.12$. If we invoked a more conservative recirculation signature,

consistent with Bergen's observations of (1) updrafts at our upwind tower, (2) downdrafts at the downwind tower, (3) $U < 0$ at the upwind tower, and (4) a near-zero U at the downwind tower (defined as having a block-average U less than the overall period average), we calculated $\tau_{\text{recir}} = 0.02$. Although both of the above classification schemes are unsophisticated, we believe they show that the wind pattern in the cutblocks was dominated by throughflow.

4. Comparisons with other experiments

In this study we were particularly interested in whether common flow patterns exist in cutblocks of different dimensions, and cutblocks having different upwind and downwind forest features. This is an important question when considering silvicultural designs that differ from the situation of our study cutblocks. When the wind statistics from our two different width cutblocks are plotted together versus x/h (Fig. 9), they show surprisingly good agreement with each other. The greatest difference was the U deceleration ($\partial U/\partial x < 0$) observed upon 'entering' the narrow cutblock, which was not seen in the wide cutblock (where, however, our anemometer spacing may have been too great to reveal this). The overall agreement in the wind statistics between the two cutblocks was surprising, given differences in upwind conditions. For instance, the narrow cutblock had an upwind forest border (entry-region) of approximately $2h$, while the wide cutblock had an entry-region border of approximately $6h$. This suggests that upwind features have a limited influence on the flow in a cutblock[2]. The agreement also shows that the effects of the downwind forest edge do not propagate very far upwind. If it is true that upwind and downwind conditions have limited influence on cutblock winds, we might then expect that wind observations from other forest-clearing interfaces would show similarities with our data.

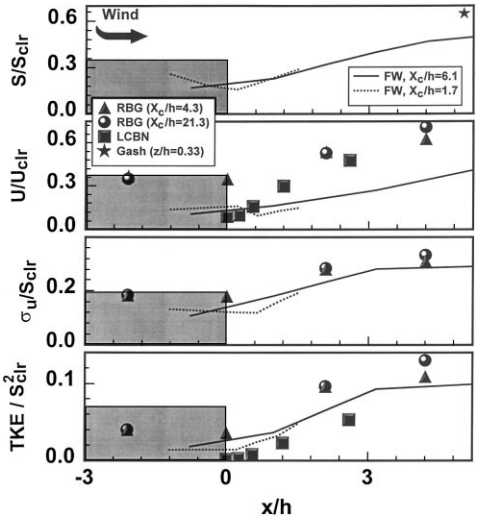

Fig. 9. Multi-experiment comparison of average cup windspeed (S), average across-cutblock velocity (U), u velocity fluctuations (σ_u), and turbulent kinetic energy (TKE), plotted versus distance from the upwind forest (x/h). These statistics are scaled on clearing values of S or U (S_{clr} and U_{clr}). Our observations, denoted FW, are shown as lines. Other observations are plotted using the symbols described in the legend: RBG denotes Raupach et al. (1987), LCBN denotes Liu et al. (1996), and Gash denotes Gash (1986).

4.1. Experiment of Gash (1986)

Gash (1986) measured winds near a forest-heath interface (the forest was a mix of pine and larch, the heath of heather and shortgrass). Because these data, which were taken mostly at a height $z/h = 0.33$, were scaled on above forest wind velocities (for which we did not have an equivalent observation), we were not able to fully compare Gash's observations with our data. We can say that Gash observed a larger S/S_{clr} at $x/h = 5$ than we found at more or less the same location at Hotchkiss (Fig. 9). We do not know if this marked difference is due to differences in forest density and/or forest architecture, upwind geometry, or place of observation. However, we do know that our values of S/S_{clr} and U/U_{clr} also stand out as low relative to other comparable data that we have examined (as will be demonstrated in the comparisons that follow).

From Gash's observations we can also surmise that a narrow quiet zone existed in the heath immediately downwind of the forest. Gash observed that both σ_u and σ_w at $x/h = 5$ were larger than values further downwind of the forest. Therefore a quiet zone, in which σ_u and σ_w were below their far-downwind

[2]However, in Part 3 of this series we describe model results which suggest that the amount of upwind forest can have a large impact on U and TKE in the cutblock.

values, must have been confined to $x/h < 5$. This is consistent with our results.

Gash's observations also raise a question about whether the winds at our reference clearing typify a 'generic' large clearing. Even as far downwind as $x/h = 40$, Gash observed $\partial S/\partial x > 0$: which suggest our observations at $x/h = 20$ have not reached an equilibrium clearing state. However, because the change in S as seen by Gash was small beyond $x/h = 20$, and because σ_u and σ_w had apparently reached an equilibrium at $x/h = 20$, we feel comfortable that our observations at $x/h \approx 20$ can be interpreted as representing the winds in a generic large clearing.

4.2. Experiment of Raupach et al. (1987)

The wind tunnel study of Raupach et al. (1987), referred to as RBG, may more easily be compared with our observations. The RBG study examined two model forest clearings ($X_c/h = 4.3$ and 21.3), bordered upwind and downwind by forest, with wind measurements at locations nearly equivalent to our observations. Their measurement at $x/h = 21.3$, at the downwind boundary of the large clearing, roughly corresponds in terms of distance downwind from the nearest shelter, to the location of our reference clearing observation (unfortunately, we must accept that this velocity is affected to some extent by the forest edge nearby). We compared our measurements with RBG values interpolated to $z/h = 0.4$.

Fig. 9 shows horizontal profiles of U/U_{clr} from the two RBG cutblocks and our two cutblocks. The similarity in wind statistics between the two so-different sized RBG cutblocks echoed the similarity we observed between our two cutblocks. However, RBG reported much higher values of U/U_{clr} than we observed. In the upwind forest they found a U/U_{clr} that was three times what we observed. These differences continued into the cutblock. We expected some differences in U/U_{clr}, given that important forest details almost certainly differed. The RBG model forest had an equivalent plant area index (PAI) of 0.5, calculated as the frontal area of the model canopy elements per unit floor area. This represents a low density forest, although RBG argued that their effective PAI was higher because the drag of their canopy elements was higher than those of a real forest (see Finnigan and Mulhearn, 1978). The aerodynamic 'density' of our forest is unknown. Sakai et al. (1997) estimated that PAI $\simeq 1$ in a leafless mixed deciduous forest. Given the substantial spruce understory at Hotchkiss, we believe our forest had a PAI of between 1 and 2, and was therefore more dense than the RBG forest. This may account in part for the lower normalised wind velocity seen in our cutblocks.

Some differences in U/U_{clr} may also be explained by errors in the RBG measurements. The hot-film anemometers used by RBG could not differentiate reversed flow, but reversal was observed visually, so that errors in their U measurements certainly occurred. We simulated a perfect hot-film sensor that measures only $|u|$, and found that this sensor would overestimate U at Hotchkiss by up to 16% in the wide cutblock and 25% in the narrow cutblock, and underestimate σ_u by up to 19%. Errors of similar magnitude may have occurred in the RBG experiment.

While there were large differences in the average wind velocity between our cutblocks and the RBG clearings, the turbulence observations were surprisingly similar (Fig. 9). Although σ_u/U_{clr} and σ_w/U_{clr} in the RBG forest were higher than we observed (perhaps the result of differences in forest structure), the in-cutblock values were in good agreement [3]. RBG observed a maximum σ_u/U_{clr} of approximately 0.3 (at $x/h = 4.2$) compared with our maximum of 0.29 (at $x/h = 5.4$), and a maximum σ_w/U_{clr} of 0.19 compared with our 0.17. RBG observed that both σ_u and σ_w fell slowly after this peak in their wide clearing.

4.3. Experiment of Liu et al. (1996)

The wind tunnel observations described by Liu et al. (1996), referred to as LCBN, were also directly comparable with our observations. LCBN looked at a forest-large clearing interface ($x/h > 22$). Velocity measurements were made in the clearing at $x/h = 22$, providing a 'clearing' velocity scale (U_{clr}) nearly matching our reference scale. We compared our wind measurements (at $z/h = 0.4$) with the closest measurement height of LCBN.

[3] We scaled σ_u, σ_w, and TKE at Hotchkiss by S_{clr}, and the RGB observations were scaled by U_{clr} (as were the LCBN observations). Since we looked at periods when V was small, the difference between the two normalisations was slight.

Fig. 9 shows horizontal profiles of U/U_{clr} from the LCBN study. The $U/U_{clr} = 0.09$ observed by LCBN at the upwind forest edge was similar to our forest observations. However, the increase in U/U_{clr} with x in the LCBN clearing was steeper than we found, so that U/U_{clr} was double our observations by $x/h \approx 3$. Again, we expected some differences in U/U_{clr} due to differences in forest structure, and the potential for hot-film errors. The LCBN forest had an equivalent PAI of 6.3, and represented a much more dense forest than ours. It is interesting that in both the RBG clearings (where we believe the forest was less dense than ours) and in the LCBN clearing (where we believe the forest was more dense than ours) the values of U/U_{clr} were larger than we observed. This suggests that differences in forest density do not explain the differences in U/U_{clr}.

Individual turbulent velocity components were not reported by LCBN, although they reported TKE and this is shown in Fig. 9. Compared with our measurements, LCBN observed lower levels of TKE at the forest edge. Some underestimation of TKE was likely due to hot-film errors near the forest edge (where at Hotchkiss we observed frequent flow reversal). However, we believe that most of the difference relative to our data was due to the very dense LCBN forest, which results in low U and TKE in the subcanopy of the upwind forest, and in the clearing immediately downwind of the forest. At locations $x/h > 1$, TKE/S^2_{clr} in our cutblocks was statistically indistinguishable from LCBN's observations.

4.4. Similarity in wind 'recovery'

We looked at a dimensionless shape factor for relative wind 'recovery' across a forest clearing [4], to focus on the spatial pattern of wind statistics across different experiments. This wind recovery factor for U was defined as

$$R_u(x) = \frac{U(x) - U_{for}}{U_{clr} - U_{for}}$$

where U_{for} was the velocity at (or near) the upwind forest edge, while U_{clr} was the reference clearing velocity (in our case measured at $x/h = 20$). Similarly, we defined a shape factor for TKE (R_{TKE}). For our the wide cutblock we assumed that U_{for} and TKE_{for} were given by their values at $x/h = -0.8$. For the narrow cutblock we assumed that U_{for} and TKE_{for} were given by their values at $x/h = 0.2$.

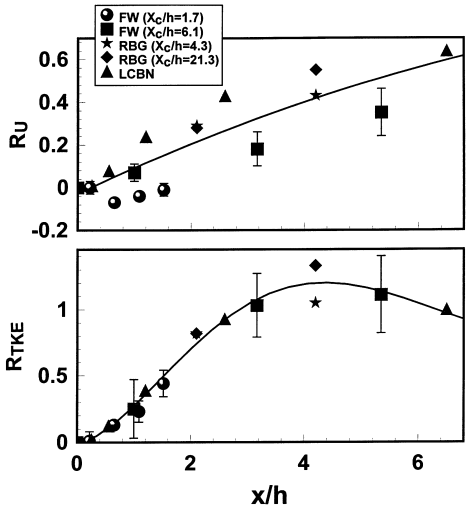

Fig. 10. Relative recovery of U (R_U) and TKE (R_{TKE}) with distance from the upwind forest edge (x/h) for several experiments. FW denotes our observations, RBG denotes Raupach et al. (1987), and LCBN denotes Liu et al. (1996).

Fig. 10 shows R_U for the different experiments. While the RBG and LCBN data were in good agreement, we observed a much lower U recovery ($\partial R/\partial x$) in our cutblocks, particularly for the narrow cutblock (where there was U deceleration with x). The scatter in R_U suggests that there is no 'universal' recovery curve for average winds across a forest clearing. We speculate that the differences in R_U were due to large differences in the pressure fields, presumably induced by differences in forest/clearing geometry (although this apparently had little influence on the TKE, as described below). In the third paper of this study (Wilson and Flesch, 1999) we show model results predicting strong 'adverse' pressure gradients across cutblocks ($\partial P/\partial x > 0$), which are sensitive to changes in the forest-clearing geometry.

In contrast to U, the different TKE observations collapsed about a 'universal' R_{TKE} curve as shown in Fig. 10 (we assumed $TKE = (2\sigma_u^2 + \sigma_w^2)/2$ in the RBG case). These experiments showed an initially rapid rise

[4] As mentioned by McNaughton (1989), it is ambiguous to speak of a wind recovery downwind of a forest – what is the wind recovering to? For our purposes, we will speak of a wind 'recovery' to conditions at our clearing location at $x/h = 20$.

in TKE with x at the upwind edge of the clearing, with TKE reaching the clearing level at $x/h \approx 3$. From Fig. 10 it appears that TKE peaked between $x/h = 4$ and 6, then fell slowly with increasing x. The fact that R_{TKE} was similar across experiments having different clearing dimensions ($X_c/h = 1.7$, 4.3, 6.1, 21.3, and >22), and different upstream forest 'entry-region' borders (2, 6, 15 and 53h), points to a limited influence of both upwind and downwind features on the *pattern* of TKE within a cutblock. We are hesitant to conclude this is universally true however, as the wind flow model described in the third paper of this series (Wilson and Flesch, 1999) predicts otherwise.

5. Conclusions

We believe a 'quiet' zone/'wake' zone picture provides a good description of the wind pattern in a forest cutblock. When the winds were oriented across the cutblock width, the quiet zone, where U and TKE were reduced from values in a large clearing, extended from $0 < x/h \leq 3$ (at our measurement height of $z/h = 0.4$). Downwind of this was a wake zone, where the TKE was above clearing values. Based on comparisons with other studies, we believe that this quiet/wake zone pattern exists across a wind range of cutblocks (with different dimensions, different upstream features, and different forest architectures).

The natural question asked by forest managers when considering shelterwood harvest designs is, how do cutblock dimensions affect wind shelter, and ultimately the windthrow of remnant spruce? Here we have considered only the case of winds oriented across the cutblock/forest strips – in our case the expected circumstance during high wind events. We believe that the pattern of average wind velocity in a cutblock will vary according to the dimensions of the cutblock (and the upwind landscape). However, beyond the complicated region near the forest edge, it appears that U increases across the cutblock monotonically. Our observations do not point to an obvious optimum cutblock width that would balance economic efficiency (i.e., larger cutblocks) and good average wind reduction (smaller cutblocks).

This is not so in terms of the turbulence. The evidence suggests that once a cutblock width exceeds 3h, remnant trees beyond $x/h = 3$ will be subject to turbulence as energetic as observed in a large clearing (for trees of height $z \approx 0.5h$). This presupposes a significant border of upwind forest (at least 2h) – the situation for all of the cutblocks/clearings studied here.

Our observations show that the extent of protection afforded by a sheltered cutblock depends on whether the focus is on the average wind velocity or turbulence. The relative importance of each in causing windthrow will depend on the frequency characteristics of the turbulence and the dynamical characteristics of the tree. This was the focus of the next phase of our work (Flesch and Wilson, 1999). However, we can conclude that effective shelter for both U and TKE seems guaranteed within three tree heights of the upwind forest edge (for trees of height $z \approx 0.5h$).

Acknowledgements

Funding for this work was provided by the Manning Diversified Forest Products Trust Fund. We are grateful for the help extended by Dr. Stan Navratil and Lorne Brace in initiating this work. A special thanks to Terry Thompson for his help in field work. The comments of an anonymous reviewer were appreciated.

Appendix

Anemometer errors

A.1 Cup anemometer errors

Comparing average cup windspeed (S) measured concurrently from cup anemometers and 3–D propeller anemometers showed cup overspeeding of up to 35% (we expected only small overspeeding from the propellers: Wyngaard, 1981). We observed increased overspeeding with increased turbulence intensity (e.g., σ_u/U), roughly as described by Kaganov and Yaglom (1976). A simple correction was used to account for overspeeding, by recalculating S as:

$$S = 0.93\, S_{\mathrm{unc}} - 0.21\ (\mathrm{ms}^{-1})$$

where S_{unc} is the uncorrected cup anemometer windspeed. This formula was given by regression of S from

the propellers and cup anemometers, and implicitly accounts for the effect of turbulent intensity – the greatest turbulent intensities occurred where windspeed was low. A better correction factor would use turbulence intensity directly, but for most S observations we did not have turbulence measurements.

A.2 Propeller anemometer errors

Propeller anemometers have two deficiencies that lead to errors in turbulence statistics: propeller stalling and poor high frequency response. Stalling was obvious at three of our locations (at $x/h = -0.8$, 1.0, 7.2 at the wide-cutblock), as showed by spikes in the velocity probability density functions (PDFs). We believe that the resulting errors were not significant: our correction schemes (e.g., 'redistributing' the spike in PDF at $u = 0$) did not significantly change the resulting statistics. This echos Horst (1973) who found stalling errors did not seriously affect commonly computed wind statistics. The poor high frequency response of the propellers was a more significant problem. Two approaches were used to estimate the frequency response errors: (1) a comparison between the propellers and a sonic anemometer, and (2) a spectral correction to the propeller velocity power spectra.

A 3–D sonic anemometer (CSAT-3, Campbell Sci.,) was temporarily co-located with a 3–D propeller anemometer at $x/h = 0.6$ in the narrow cutblock ($z/h = 0.4$), and the u and w velocity statistics compared. We focused on two 30 min periods (where $U > |V|$ and $\sigma_u > 0.5$ m s^{-1}). We found:

- the average U_{prop}/U_{sonic} was 1.04; the average $\sigma_{u\_prop}/\sigma_{u\_sonic}$ was 0.99;
- the average of $|W_{prop} - W_{sonic}|$ was 0.015 m s^{-1}; the average $\sigma_{w\_prop}/\sigma_{w\_sonic}$ was 0.88;
- the average of $|Sk_{u\_prop} - Sk_{u\_sonic}|$ was 0.17; the average Kt_{u_prop}/Kt_{u_sonic} was 1.14;
- the average of $|Sk_{w\_prop} - Sk_{w\_sonic}|$ was 0.35; the average Kt_{w_prop}/Kt_{w_sonic} was 1.69.

The agreement between the two anemometers was excellent for u statistics. As expected, the agreement in w statistics was worse. We also found disappointing agreement in v (e.g., $\sigma_{v\_prop}/\sigma_{v\_sonic} = 0.86$), which we partially blame on flow interference caused by our anemometer setup.

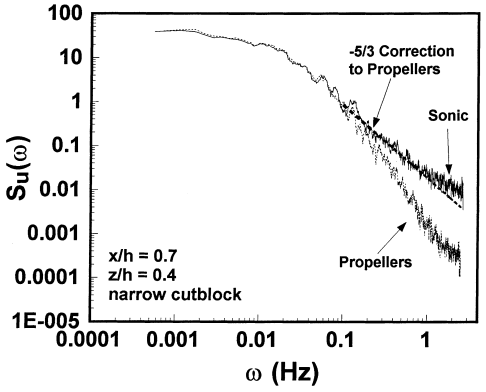

Fig. 11. Power spectrum of u (S_u) versus frequency (ω) for a single 30 min period, during which there were simultaneous observations from a 3–D propeller and sonic anemometer. Also show is a −5/3 correction for the propeller spectrum.

We also considered a 'spectral' correction to the propeller σ_u, σ_v, and σ_w values. The power spectra of velocity (S_u, S_v, S_w) were expected to show the theoretical −5/3 'fall-off' with frequency (ω) in the inertial subrange: e.g., $S_u(\omega) \propto \omega^{-5/3}$ (see Stull, 1988) [5]. We observed that at frequencies above 0.1–0.3 Hz, the propeller spectra departed from a −5/3 fall-off (Fig. 11). The propeller power spectra were extended along a −5/3 fall-off (for $\omega > 0.1$ Hz), and 'corrected' velocity variances were recalculated at all cutblock locations. This indicated that the propellers underestimated σ_u and σ_v by 1.5 to 4%, and underestimated σ_w by 6 to 10%.

We believe that the propellers gave reasonably accurate measurements of the turbulent statistics within the forest cutblocks, particularly for u and v. On this basis we decided not to correct the velocity statistics, recognizing that w turbulence statistics are in error, and that TKE was likely underestimated by between 5 and 10%.

References

Amiro, B.D., 1990. Comparison of turbulence statistics within three boreal forest canopies. Boundary-Layer Meteorol. 51, 99–121.

[5] Although this seems reasonable within the cutblock, it is questionable within the forest where vegetation may 'short-circuit' the normal energy cascade (Baldocchi and Meyers, 1988).

Baldocchi, D.D., Meyers, T.P., 1988. A spectral and lag-correlation analysis of turbulence in a deciduous forest canopy. Boundary-Layer Meteorol. 45, 31–58.

Baldocchi, D.D., Meyers, T.P., 1989. The effects of extreme turbulent events on the estimation of aerodynamic variables in a deciduous forest canopy. Agric. For. Meteorol. 48, 117–134.

Bergen, J.D., 1975. Air movement in a forest clearing as indicated by smoke drift. Agric. Meteorol. 15, 165–179.

Finnigan, J.J., Mulhearn, P.J., 1978. Modelling waving crops in a wind tunnel. Boundary-Layer Meteorol. 14, 253–277.

Finnigan, J.J., Raupach, M.R., 1987. Transfer processes in plant canopies in relation to stomatal characteristics. In: E. Zeiger, G.D. Farquhar, I.R. Cowan, (Eds.), Stomatal Function, Stanford University Press.

Flesch, T.K., Wilson, J.D., 1999. Wind and remnant tree sway in forest cutblocks II. Relating measured tree sway to wind statistics., Agric. For. Meteorol, in press.

Gash, J.H.C., 1986. Observations of turbulence downwind of a forest-heath interface. Boundary-Layer Meteorol. 36, 227–237.

Horst, T.W., 1972. A computer algorithm for correcting non-cosine response in the Gill anemometer. Pacific Northwest Laboratory Annual Report for 1971 to the USAEC Division of Biology and Medicine, vol. 2, Physical Sciences part 1, Atmospheric Sciences, BNWL–1651–1. Battelle, Pacific Northwest Laboratories, Richland, Wash.

Horst, T.W., 1973. Corrections for response errors in a three-component propeller anemometer. J. Appl. Meteorol. 12, 716–725.

Kaganov, E.I., Yaglom, A.M., 1976. Errors in wind-speed measurements by rotation anemometers. Boundary-Layer Meteorol. 10, 15–34.

Liu, J., Chen, J.M., Black, T.A., Novak, M.D., 1996. E-ω modelling of turbulent air flow downwind of a model forest edge. Boundary-Layer Meteorol. 77, 21–44.

McNaughton, K.G., 1989. Micrometeorology of shelter belts and forest edges. Phil. Trans. R. Soc. Lond. B 324, 351–368.

Navratil, S., Brace, L.G., Sauder, E.A., Lux, S., 1994. Silvicultural and harvesting options to favor immature white spruce and aspen regeneration in boreal mixedwoods. Natl. Resour. Can. Can. For. Serv. Northwest Reg., Edmonton, Alberta, Information Report NOR–X–337.

Raine, J.K., Stevenson, D.C., 1977. Wind protection by model fences in a simulated atmospheric boundary layer. J. Industrial Aerodynamics. 2, 159–180.

Raupach, M.R., Bradley, E.F., Ghadiri, H., 1987. Wind tunnel investigation into the aerodynamic effect of forest clearing of the nesting of Abbott's Booby on Christmas Island. Progress Report, CSIRO Division of Environmental Mechanics, GPO Box 821, Canberra, ACT 2601, Australia.

Sakai, R.K., Fitzjarrald, D.R., Moore, K.E., 1997. Detecting leaf area and surface resistance during transition seasons. Agric. For. Meteorol. 84, 273–284.

Stull, R.B., 1988. An Introduction to Boundary Layer Meteorology. Kluwer Academic Publishers, Dordrecht, 666 pp.

Weiss, A., Allen, L.H., 1976. Air-flow patterns in Vineyard Rows. Agric. Meteorol. 16, 329–342.

Wilson, J.D., Flesch T.K., 1999. Wind and remnant tree sway in forest cutblocks III: a wind flow model to diagnose spatial variation., Agric. For. Meteorol, in press.

Wyngaard, J.C., 1981. Cup, propeller, vane, and sonic anemometers in turbulence research. Ann. Rev. Fluid Mech. 13, 399–423.